Science Advances
AAAS

Supplementary Materials for

Time-restricted feeding prevents deleterious metabolic effects of circadian disruption through epigenetic control of β cell function

Matthew R. Brown, Satish K. Sen, Amelia Mazzone, Tracy K. Her, Yuning Xiong, Jeong-Heon Lee, Naureen Javeed, Christopher S. Colwell, Kuntol Rakshit, Nathan K. LeBrasseur, Alexandre Gaspar-Maia, Tamas Ordog, Aleksey V. Matveyenko*

*Corresponding author. Email: matveyenko.aleksey@mayo.edu

Published 15 December 2021, *Sci. Adv.* **7**, eabg6856 (2021)
DOI: 10.1126/sciadv.abg6856

The PDF file includes:

Supplementary Text
Figs. S1 to S9
Legend for data S1

Other Supplementary Material for this manuscript includes the following:

Data S1

Supplementary Text

RNA-sequencing bioinformatics

RNA-sequencing reads were first mapped to the mm10 or rn6 build of the mouse and rat reference genome, respectively, using HISAT v2.1.0 with default settings. FeatureCounts v2.0.0 from the Subread package was used to count mapped gene-level reads. Gene count matrices were uploaded into the edgeR v3.28.1 package and normalized to counts per million (CPM) reads using the default Trimmed Mean of M-values (TMM) method. For both INS-1 832/13 β-cell and mouse islet samples, genes that were expressed at a level ≥1 CPM in ≥50% of samples were included in downstream analysis. To identify circadian transcripts in mouse islet samples, normalized count matrices were imported into MetaCycle v1.5.0 and circadian rhythmicity was determined by ARSER method with default settings (period=20-28h) (*29, 30*). ARSER was used due to its noted superior performance and normal statistical distribution under equivalent experimental design conditions (*31*). Genes were considered significantly rhythmic at a false discovery rate (FDR; Benjamini and Hochberg) ≤ 0.10. Significantly rhythmic genes were subjected to biological pathway enrichment using WebGesalt v2019 and HOMER v4.11.1. To assess potentially cis-regulatory elements mediating circadian control of transcription, the peak phase of rhythmic genes was obtained from ARSER and binned into 4h intervals (± 2h from center). Each subset of genes was inputted into i-cisTarget 2015 for cis-regulatory enrichment analysis using default settings (±10kb from transcriptional start site). Normalized enrichment scores of transcription factor motifs from the Catalog of Inferred Sequence Binding Preferences (cis-BP) mouse motif set were retained for analysis. To identify differential expressed genes in transfected INS-1 832/13 β-cells, normalized gene count matrices were subjected to differential analysis using edgeR's default Fisher's exact test and considered statistically significant at a

FDR<.05 (Benjamini-Hochberg method) and a fold change > 1.2. Differentially expressed genes were subjected to biological pathway enrichment using WebGesalt v2019 and HOMER v4.11.1. Gene-set enrichment analysis v4.0.1 (GSEA) was used to calculate enrichment of 'de-novo' gene-sets against a pre-ranked gene list of calculated fold changes in INS-1 832/13 β-cells, using default settings.

Bulk ATAC-sequencing bioinformatics

Bulk ATAC-sequencing reads were first mapped to the mm9 build of the mouse reference genome using the Burrows-Wheeler Aligner v0.7.16 with default settings. Picard v2.21.6 was used to remove PCR duplicates and which were subsequently removed by Samtools v1.9 along with mitochondrial and multi-mapping reads To call peaks, we used MACS2 v2.2.7.1 on merged replicates with the following settings: -f BEDPE -g mm --keep-dup all --SPMR -q 0.05. Peaks with an FDR <0.05 were retained following removal of peaks overlapping mm9 blacklisted regions. Bedtools v2.27.1 was used to perform genomic arithmetic on called peaks. All samples achieved a fraction of reads in peaks (FRIP) score ≥50%. The Integrative Genomics Viewer v2.6.3 was used to view ATAC-seq coverage tracks. Differentially accessible chromatin regions of MACS2 called peaks were determined by DiffBind v2.14.0 and considered differentially accessible with a fold change > 1.5 and FDR<0.1. Peak classification was performed by ChIPseeker v1.22.1, motif enrichment was performed using i-cisTarget 2015 and HOMER's findMotifsGenome.pl function, and gene ontology determined by GREAT 4.0.41 all using default settings. To predict sites of transcription factor binding, ATAC-seq samples were corrected for Tn5 bias and transcription factor footprints for each condition were identified by TOBIAS v0.11.6 using default settings and subsequently visualized using deepTools v2.0 (*37*,

45). Diurnal differential transcription factor footprinting was performed by the Bivariate Genomic Footprinting R package (BagFootR v0.9.3) following cut bias correction using default settings and default cis-BP motif set (*36*). Transcription factors were considered diurnally active at an FDR<0.05 using the Hotelling's T squared test.

Single cell ATAC-seq bioinformatics

Raw base cell files (BCL; Illumina) were demultiplexed into FASTQ file format by Cell Ranger ATAC v1.2.0 using the cellranger-atac mkfastq function (10X Genomics). ScATAC-seq accessibility counts for each library were obtained using the cellranger-atac count function against the mm10 reference genome. Aligned sequenced fragment files generated by Cell Ranger were then imported into ArchR v1.0.0 for quality control and sample processing (*40*). Low quality cells were filtered if < 1000 unique fragment counts were detected or given a TSS enrichment score < 10. Predicted doublets were inferred using ArchR's addDoubletScores algorithm which synthesizes pseudo-doublets by in silico mixing of cellular populations followed by comparison with experimental data. Cells were then filtered using both the default filterDoublets function and given > 4000 unique fragment counts in TSS regions. Dimensionality reduction of the term frequency-inverse document frequency (TF-IDF) normalized scATAC-seq data (16470 cells) was performed using iterative Latent Semantic Indexing (LSI) using genome-wide 500bp tiling of accessible chromatin regions (iterations=2, varFeatures=20000, resolution=0.2, dimsToUse=1:15). The data was then clustered using Seurat's FindClusters algorithm (resolution=1.2) and visualized using Uniform Manifold Approximation and Projection (UMAP) embedding (nNeighbors=40, minDist=0.5, metric=cosine). Gene activity scores were calculated using ArchR's gene scoring model which considers both the accessibility

within a gene loci and exponentially weighted distal elements based on distance to a gene's TSS. Gene activity scores for individual cell were visualized on UMAP embeddings following markov affinity-based graph imputation of cells. Marker features of each cluster were quantified using ArchR's getMarkerFeatures algorithm. Cell-specific clusters were then manually assigned, as previously performed for scATAC-seq protocols (*38, 41*), to endocrine or non-endocrine cell type by enrichment of canonical endocrine markers (NK2 homeobox 2 (*Nkx2.2*), paired box protein 6 (*Pax6*), and *Neurod1*. Endocrine cell types were sub-classified into β-cell (*Ins1, Ins2, Nkx6.1,* MAF bZip transcription factor A (*Mafa*), insulin amyloid polypeptide (*Iapp*)), α-cell (*Gcg,* aristaless Related Homeobox (*Arx*), iroquois homeobox factor 1 (*Irx1*), MAF bZip transcription factor B (*Mafb*)), δ-cell (*Sst,* peptide YY (*Pyy*) *and* hematopoietically-expressed homeobox protein (*Hhex*)), and γ-cell clusters (*Ppy,* tetraspanin 8 (*Tspan8*), *Pyy)*, while non-endocrine cells were classified into immune (cluster of differentiation 74 (*Cd74*),C-C motif chemokine ligand 3 (*Ccl3*),histocompatibility 2, class 2 antigen E beta 2 (*H2-Eb2*)), endothelial (kinase insert domain receptor (*Kdr*),SRY-box transcription factor 7 (*Sox7*),cluster of differentiation 34 (*Cd34*)), and stellate cell clusters (heart and neural crest derivatives expressed 2 (*Hand2*), collagen type VI alpha 1 chain (*Col6a1*),anoctamin 1 (*Ano1*)). Clusters that had enrichment of endocrine and non-endocrine markers (e.g. *Kdr* and *Ins1*) or multiple endocrine cell-specific makers (e.g. *Ins1* and *Gcg*) were considered unclassified as noted in other scATAC-seq protocols and are likely unfiltered doublets (*41*). Following cell type identification, peaks were called from pseudo-bulk clustered cell-types using MACS2 v2.2.7 with the default ArchR settings --shift 75 --extsize 150 --nomodel --nolambda. To identify diurnal differences in β-cell transcription factor motif activity, β-cells were diurnally grouped by treatment condition and motif deviation score was calculated by ChromVar against a GC-content and fragment depth

corrected background peak set using ArchR's default cis-BP motif set (*42*). Transcription factor activity scores were imputed by markov affinity-based graph imputation of cells (*39*) and considered diurnally active at an FDR<0.05 using Wilcoxon Rank sum test. β-cells were then classified by mean PAR bZip (DBP, HLF, and TEF) activity Z-score from low activity (0-25th percentile) to intermediate (25-75th percentile) and high activity (75-100th percentile). The classified cells were then subjected to pseudotime trajectory analysis using ArchR's addTrajectory algorithm with default settings (40). The top 10% of gene scores and top 5% of accessible chromatin regions which varied across pseudotime were identified and plotted. Genes and chromatin regions with maximal activity/accessibility between pseudotime 5-50 were considered enriched in PAR bZip low cells, while pseudotime 70-100 was considered for PAR bZip high cells. Genes and chromatin regions were subjected to gene ontology enrichment analysis using WebGesalt2019 and GREAT v4.0.4.

ChIP-seq Informatics

ChIP-sequencing reads were mapped to the rn6 build of the rat reference genome using HISAT v2.1.0 with default settings. DBP peaks were called using the MACS2 v2.2.7 algorithm using a false discovery rate of 1%. Peak classification, motif enrichment, and gene ontology were performed by HOMER v4.11.1 using default settings. For identification of DBP binding sites within active enhancer regions, processed H3K27ac ChIP-seq data from INS-1 cells was obtained from GSE126556 (*44*). Bedtools was utilized to identify DBP peaks <3kb from active enhancer regions. Peaks ≤3kb from HOMER defined transcriptional start sties were considered proximal enhancers, with >3kb considered distal. Processed mouse islet ChIP-seq data of FOXO1 and H3K27ac was downloaded from GSE131947 (*55*). The integrative genomics viewer

was used to visualize ChIP-seq coverage tracks, while deepTools was used to generate heatmaps and profiles of DBP binding (*45*). To assess the expression of DBP target genes in human islets obtained from non-diabetic and type 2 diabetic patients, five gene arrays (GSE38642 (*46*), GSE 25724 (*47*), GSE20966 (*48*), GSE76894 (*49*), and GSE76895 (*49*)) and two RNA-seq studies (GSE159984 (*51*) and GSE164416 (*52*)) were downloaded from the NIH gene expression omnibus, each containing at least 5 non-diabetic and 5 type 2 diabetic donors. The gene arrays were processed as described previously (*50*). For GSE159984, the differential gene expression was downloaded from the GEO website, while GSE164416 was processed using edgeR's default Fisher's exact test as described above. DBP binding sites in active enhancer regions were annotated and genes were lifted over from rat to human orthologues using Biomart. DBP target genes mapping to KEGG pathways regulating circadian rhythms, insulin secretion, protein processing in the endoplasmic reticulum, and protein export were retained, provided they were probed in >50% of gene array studies. For the meta-analysis of differentially expressed DBP targets in each study, a vote counting approach was utilized with a fold change and false discovery rate cutoff of ≥ 1.2 and ≤ 0.25, respectively.

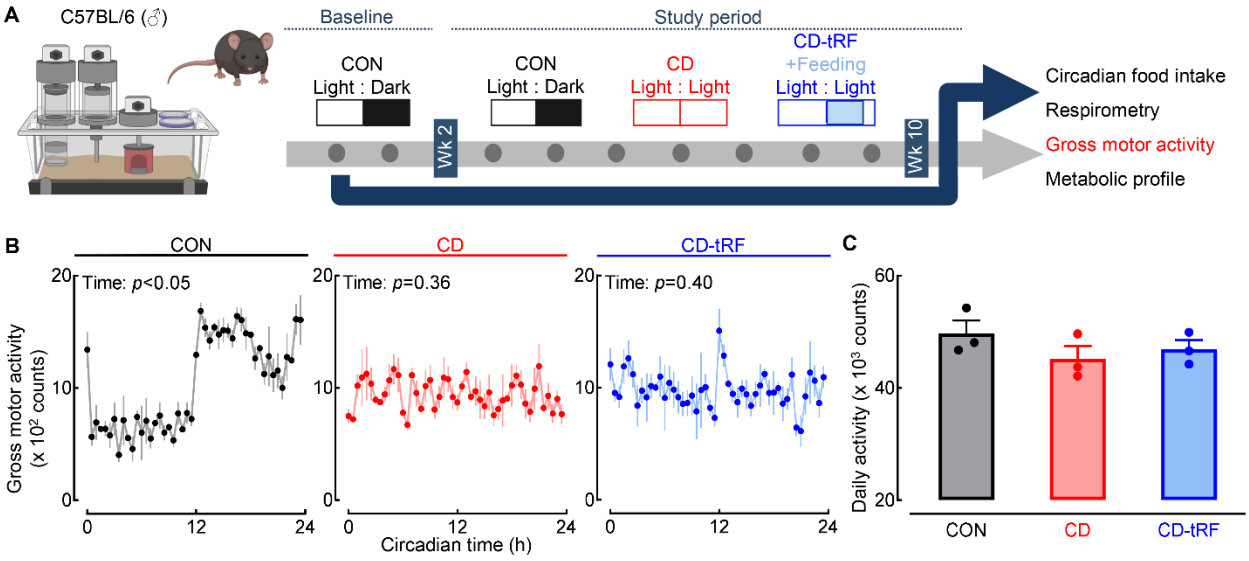

Fig. S1. Effects of time-restricted feeding on motor activity in mice exposed to global circadian disruption. (A) Overview of study design. Experimental parameters assessed and displayed in the figure are highlighted in red. **(B)** Average 24 hour circadian motor activity binned into 30-minute intervals in CON (black), CD (red), and CD-tRF (blue) mice (repeated measures one-way Anova, effect of time; n=3 mice per condition). **(C)** Total daily (24 hour) activity in CON, CD and CD-tRF mice (n=3 per group). All values represent mean ± SEM.

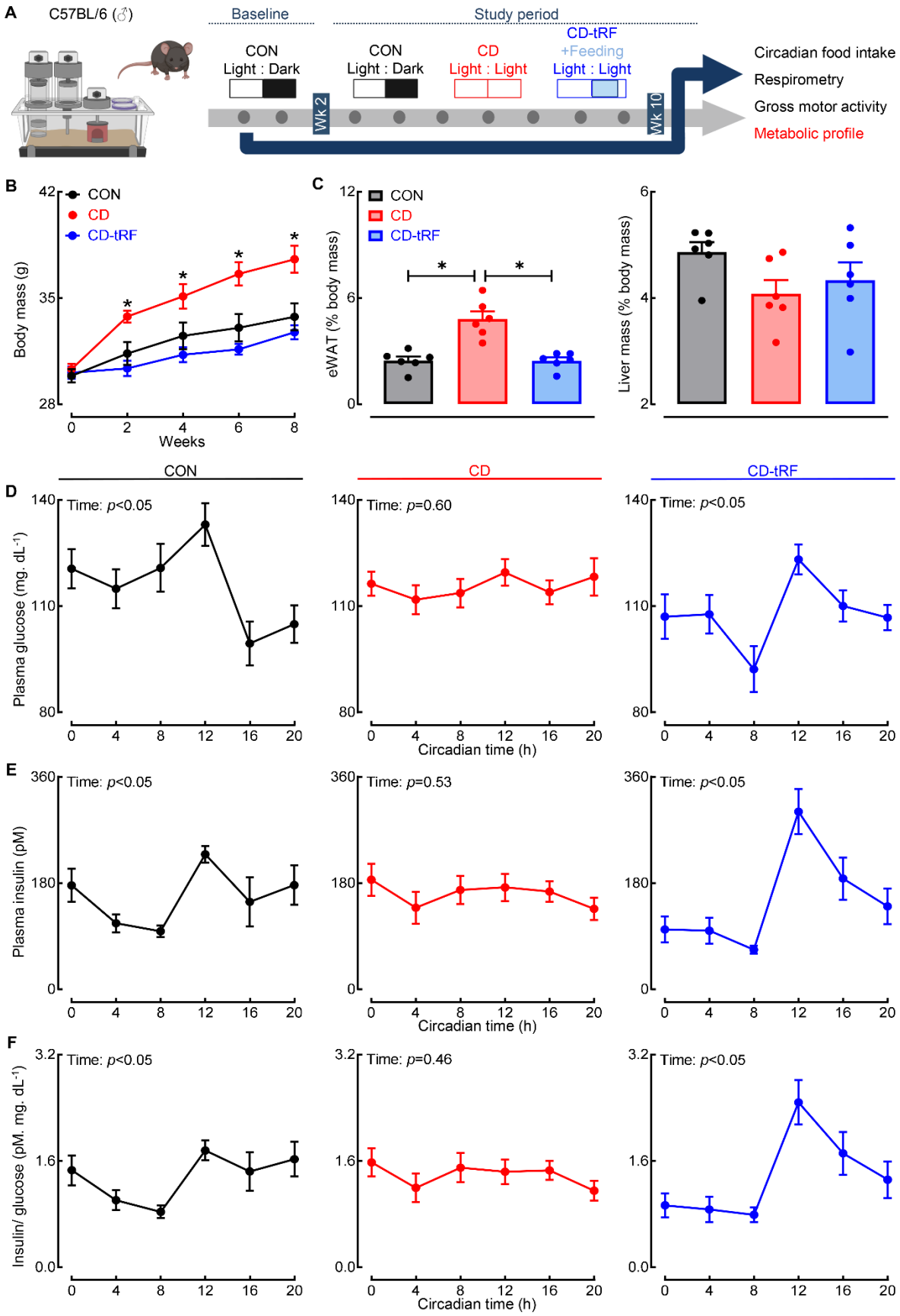
A
C57BL/6 (♂)
Baseline
Study period
CON
Light : Dark
CON
Light : Dark
CD
Light : Light
CD-tRF
+Feeding
Light : Light
Wk 2
Wk 10
Circadian food intake
Respirometry
Gross motor activity
Metabolic profile
B
CON
CD
CD-tRF
Body mass (g)
Weeks
C
eWAT (% body mass)
Liver mass (% body mass)
D
Plasma glucose (mg. dL-1)
Time: p<0.05
Time: p=0.60
Time: p<0.05
Circadian time (h)
E
Plasma insulin (pM)
Time: p<0.05
Time: p=0.53
Time: p<0.05
F
Insulin/ glucose (pM. mg. dL-1)
Time: p<0.05
Time: p=0.46
Time: p<0.05

Fig. S2. Effects of time-restricted feeding on body mass and plasma glucose/insulin concentrations in mice exposed to global circadian disruption. (A) Overview of study design. Experimental parameters assessed and displayed in the figure are highlighted in red. **(B)** Average bi-weekly body mass of CON, CD, and CD-tRF mice over 8-week experimental period. *$p<.05$ denotes statistical significance (two-way Anova with Tukey post-hoc test; n=6 per group). **(C)** Average final epididymal white adipose tissue mass (left) and liver mass (right) normalized to total body mass of CON, CD, and CD-tRF mice. *$p<.05$ denotes statistical significance (one-way Anova with Tukey post-hoc test; n=6 per group). **(D-F)** Average plasma glucose **(D)**, plasma insulin **(E)**, and insulin-to-glucose ratio **(F)** sampled every 4h from CT0 to CT20 in CON (grey), CD (red) and CD-tRF (blue) mice (repeated measures one-way Anova, effect of time; n=9-12 per group). All values represent mean ± SEM.

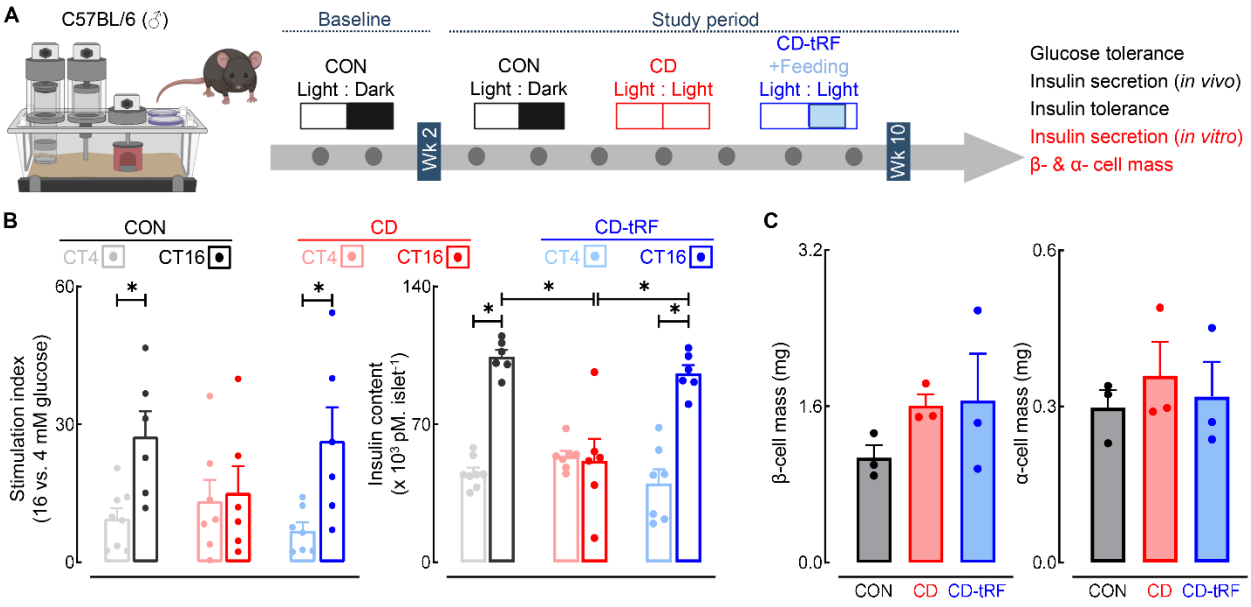

Fig. S3. Effects of time-restricted feeding on in vitro β-cell function and β/α-cell mass in mice exposed to global circadian disruption. (A) Overview of study design. Parameters displayed in the figure are highlighted in red. **(B)** Diurnal glucose-stimulated insulin secretion performed at CT4 and CT16 time points in CON (grey/black), CD (pink/red) and CD-tRF (light blue/dark blue) islets. Glucose-stimulated insulin secretion is expressed as the ratio of insulin secretion at hyperglycemic 16mM glucose to basal insulin secretion at 4mM glucose (left). Total diurnal islet insulin content measured at CT4 and CT16 time points in CON (grey/black), CD (pink/red) and CD-tRF (light blue/dark blue) islets normalized to total islet number (right). *p<.05 denotes statistical significance (unpaired, two-tailed Student's t-test for intragroup comparison and one-way Anova with Tukey correction for multiple comparison for intergroup comparison; n=6-8 independent experiments per group). **(C)** Average β-cell (left) and α-cell (right) mass of CON, CD, and CD-tRF pancreata. (p>.05; one-way Anova with Tukey post-hoc test; n=3 pancreata per group). All values represent mean ± SEM.

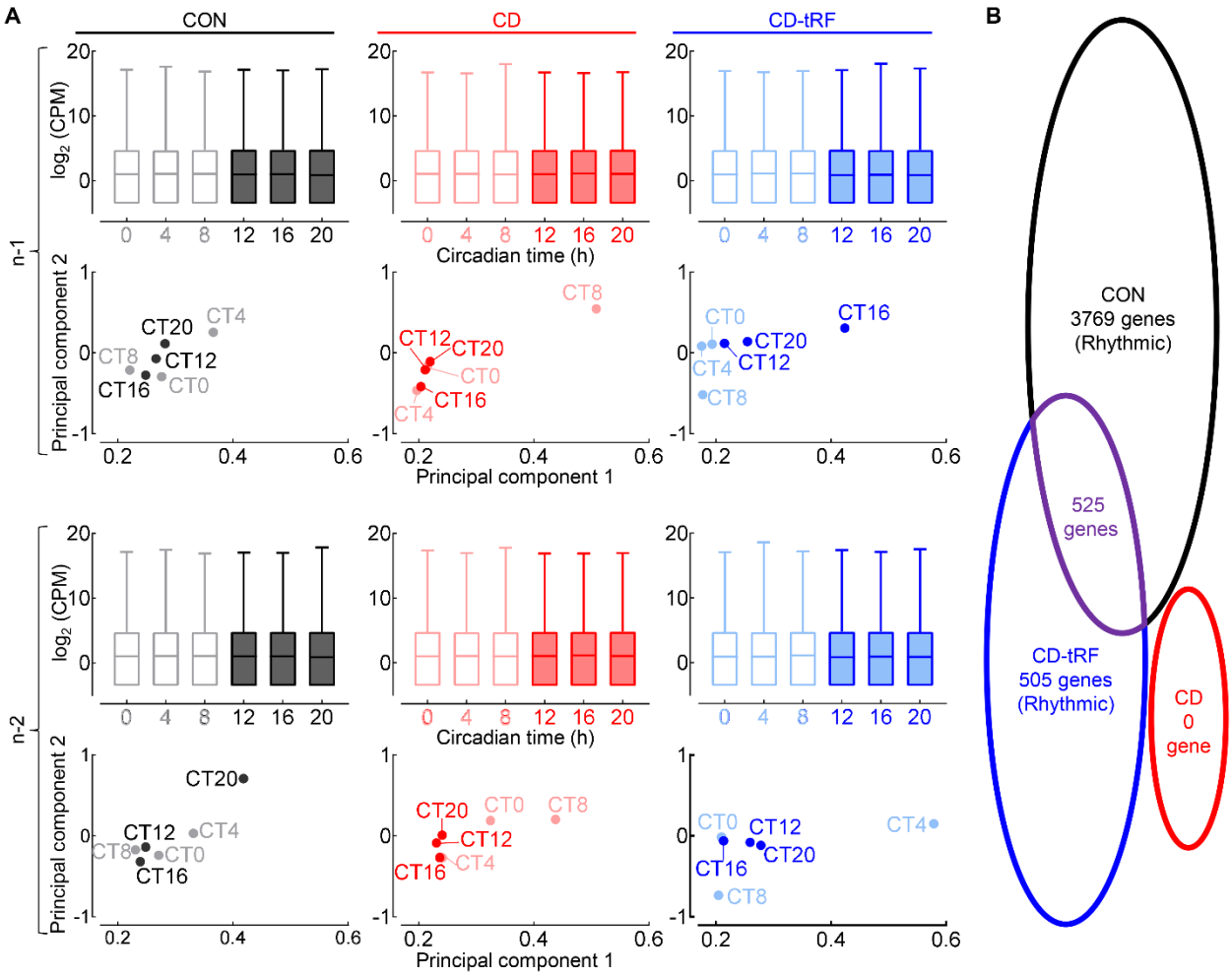

Fig. S4. Circadian RNA-sequencing of pancreatic islets from CON, CD, and CD-tRF mice. **(A)** Log_2 normalized mean gene expression expressed as counts per million reads (CPM) in two independent replicates of CON (grey/black), CD (pink/red), and CD-tRF (light blue/dark blue) samples collected every 4h starting from CT0 (n=12 samples per group). Values expressed as mean ± min/max log2 CPM (top). Principal component analysis (PCA) illustrating principal component analysis (1st and 2nd PCs) of global transcriptome for CON (grey/black), CD (pink/red), and CD-tRF (light blue/dark blue) samples (bottom). **(B)** Venn diagram highlighting number of transcripts with a significant circadian rhythmicity in CON, CD, and CD-tRF islet transcriptomic samples (FDR<.1, Benjamini and Hochberg method).

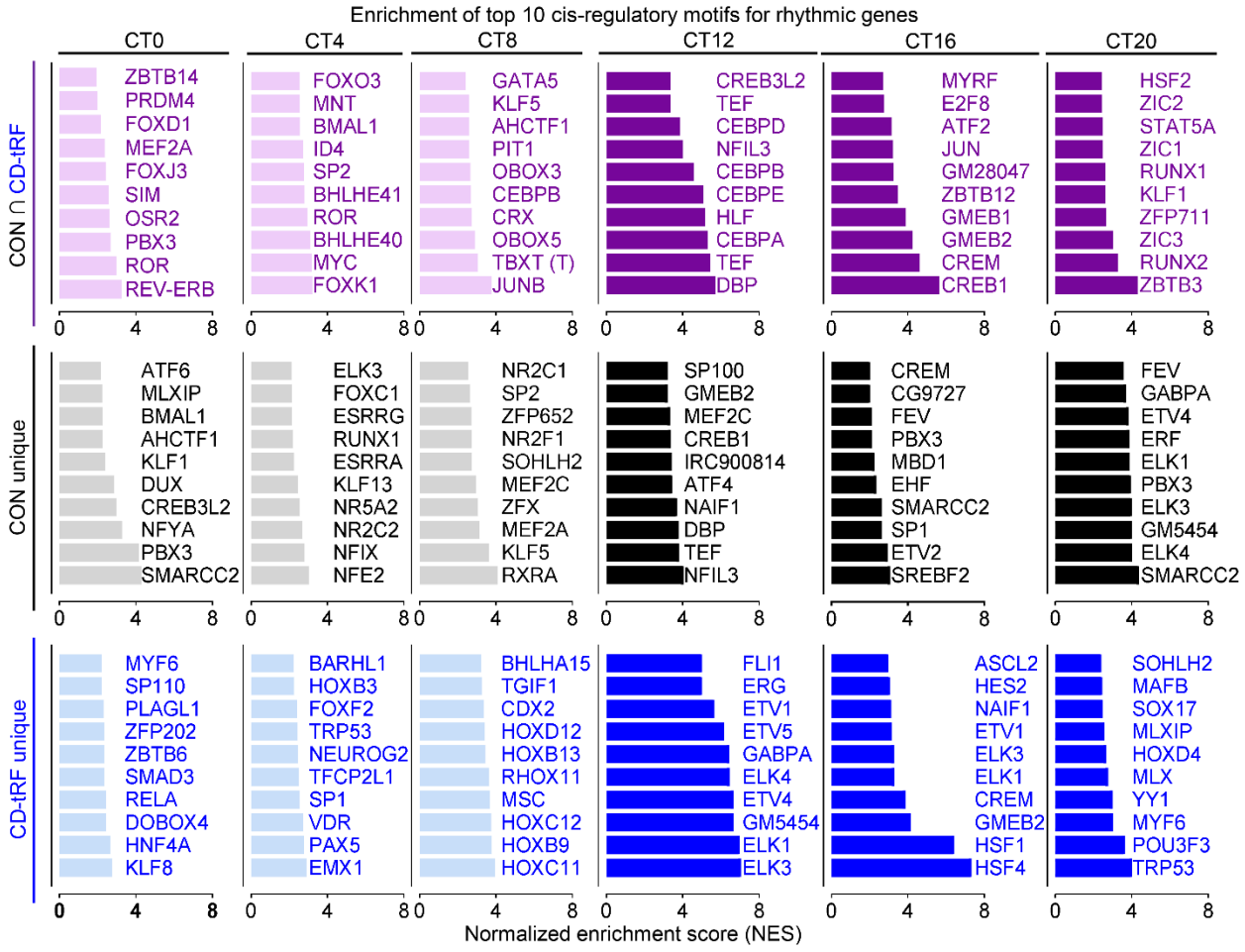

Fig. S5. Cis-regulatory motif enrichment of rhythmic genes from CON and CD-tRF pancreatic islets. Graphs representing predicted i-Cis Target enrichment of the top 10 regulatory motifs (ranked by Z-normalized enrichment score) in cis-regulatory elements of genes with a peak phase centering at the indicated circadian time common to CON and CD-tRF islets (top; grey), unique to CON (middle; black), and unique to CD-tRF (bottom; blue).

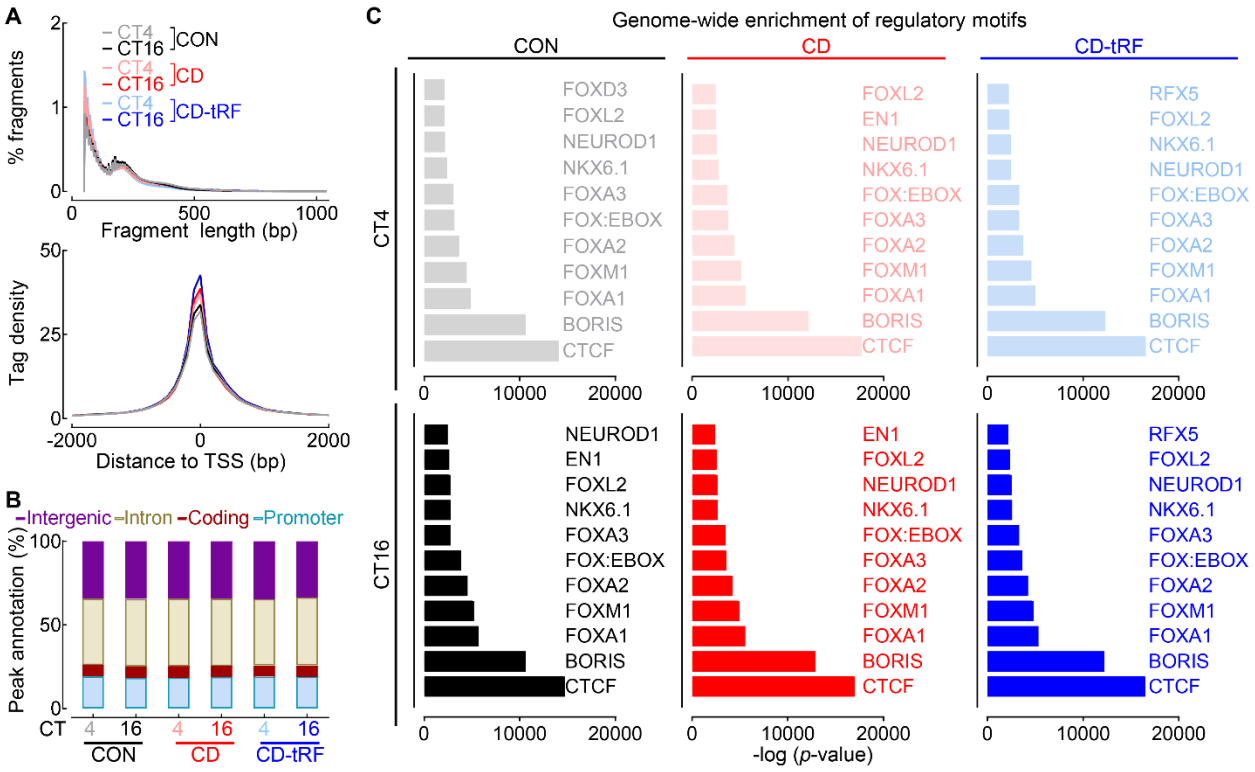

Fig. S6. Diurnal ATAC-sequencing of pancreatic islets from CON, CD, and CD-tRF mice.

(A) Representative DNA fragment size distribution of CON (grey/black), CD (pink/red), and CD-tRF (light blue/dark blue) samples isolated at CT4 and CT16 normalized to a percentage of total DNA fragment number (top). Transcription Start Site (TSS) enrichment score (signal-to-background ratio) of CON (grey/black), CD (pink/red), and CD-tRF (light blue/dark blue) samples at CT4 and CT16 (bottom). **(B)** Annotation of accessible chromatin regions to intergenic, coding, intronic, or promoter regions in the genome, normalized to total peak number in CON, CD, and CD-tRF samples at CT4 and CT16. **(C)** Top 10 known HOMER motifs, ranked by –log of p-value, enriched globally at accessible chromatin regions in CON (grey/black), CD (pink/red), and CD-tRF (light blue/dark blue) samples at CT4 and CT16.

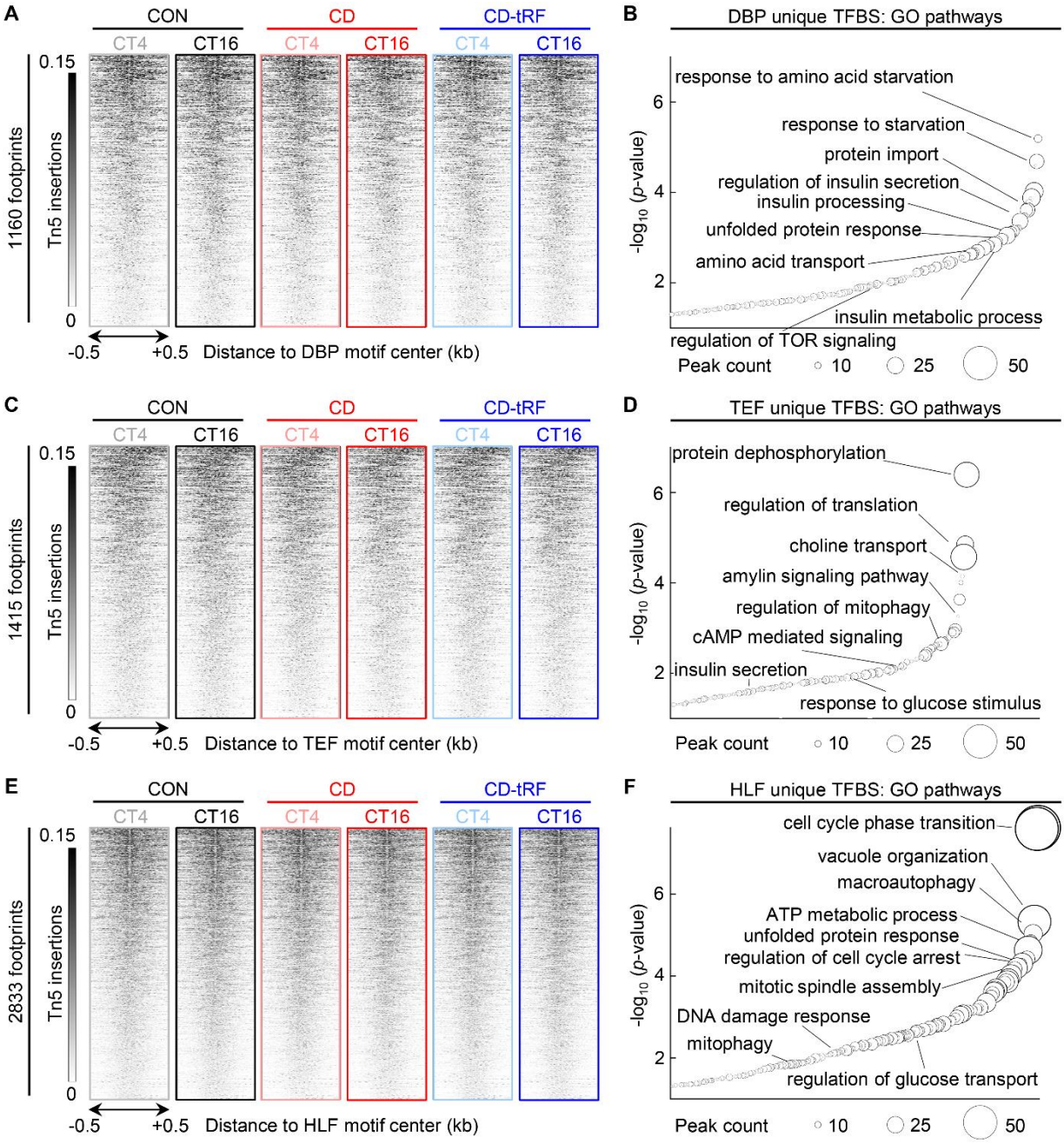

Fig. S7. Digital genomic footprinting reveals unique roles for PAR bZip transcription factors: DBP, TEF, and HLF, as potential regulators of islet function. (A, C, E) ATAC-seq signal in CON, CD, and CD-tRF sampled at CT4 and CT16 from unique DBP **(A)**, TEF **(C)**, HLF **(E)** footprints detected in CON and CD-tRF conditions. Signal is normalized to reads per genomic content and is plotted ±0.5kb from motif center. Shaded, dark regions represent areas of

accessible chromatin. **(B, D, F)** Enriched GO: Biological Process pathways annotated from unique DBP **(B)**, TEF **(D)**, and HLF **(F)** footprints. Key pathways regulating maintenance of β-cell function and survival are highlighted.

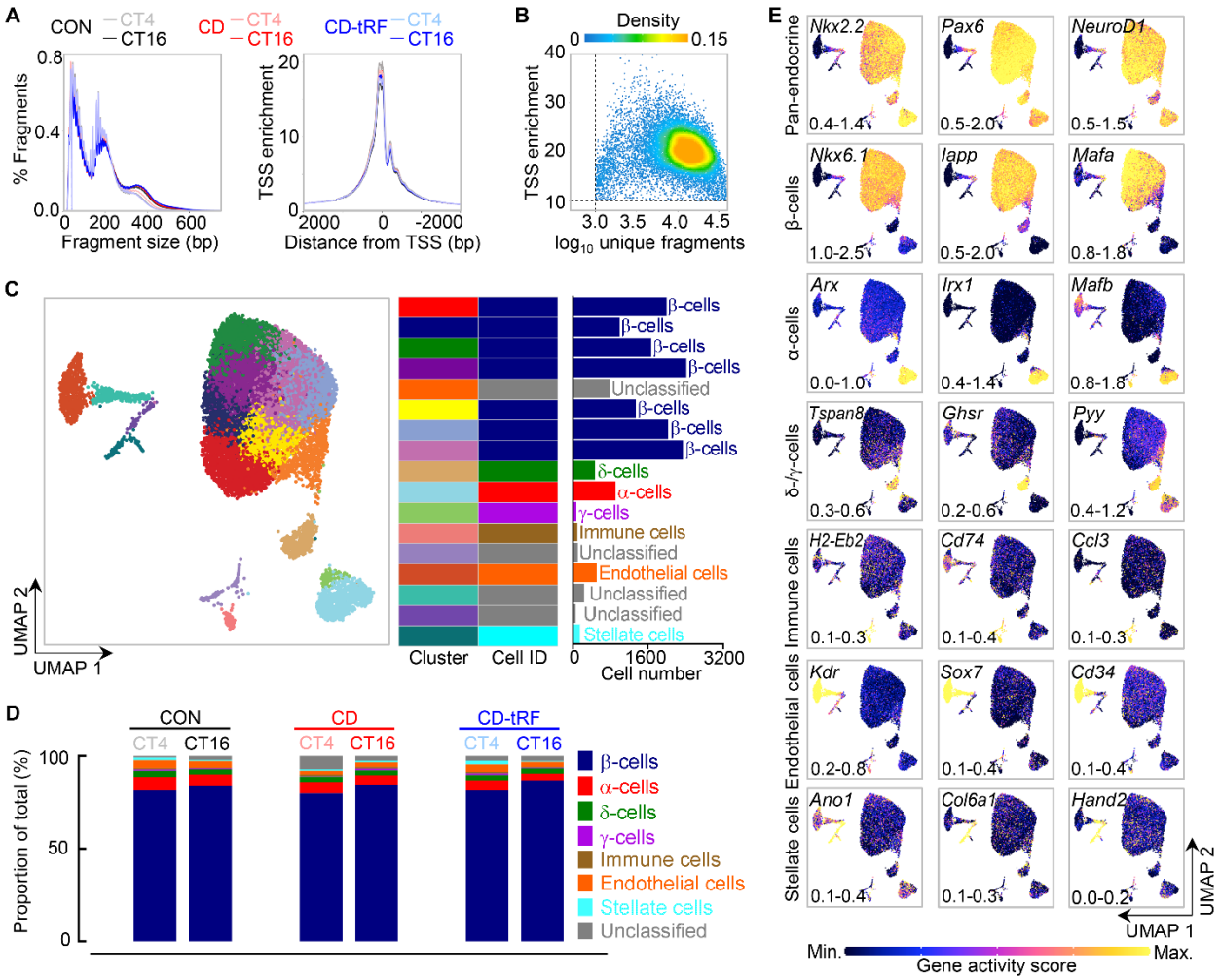

Fig. S8. Diurnal single cell ATAC-sequencing (scATAC-seq) of pancreatic islets from CON, CD, and CD-tRF mice. (A) Representative DNA fragment size distribution of CON (grey/black), CD (pink/red), and CD-tRF (light blue/dark blue) islet single cell samples obtained at CT4 and CT16 and normalized to a percentage of total DNA fragment number prior to quality control adjustment (left). Transcription Start Site (TSS) enrichment score (signal-to-background ratio) of CON (grey/black), CD (pink/red), and CD-tRF (light blue/dark blue) scATAC-seq samples obtained at CT4 and CT16 prior to quality control adjustment (right). **(B)** Heatmap representing relationship between TSS enrichment and unique DNA fragment number in captured cells following quality control adjustment. Each dot represents one cell with the dot

color representing the density of cells (n=16470) associated with a given DNA fragment number and TSS enrichment. **(C)** UMAP of scATAC-seq data from CON, CD, and CD-tRF islet samples isolated at CT4 and CT16. Each dot represents a cell (n=16470) with distinct colors for each of the 17 identified cell clusters (left). Classification of cell types by cluster and identification with corresponding quantification of total cell number per cluster (right). **(D)** Quantification of the proportion of cell types identified by sample normalized to the total number of cells captured per sample in CON, CD, and CD-tRF samples from CT4 and CT16. **(E)** UMAP of gene activity scores for canonical cell markers for each cell type identified. Range of gene activity scores plotted is noted in the bottom left corner of each UMAP. Yellow represents high activity (open chromatin) at noted gene loci, while blue/purple represents low activity (closed chromatin).

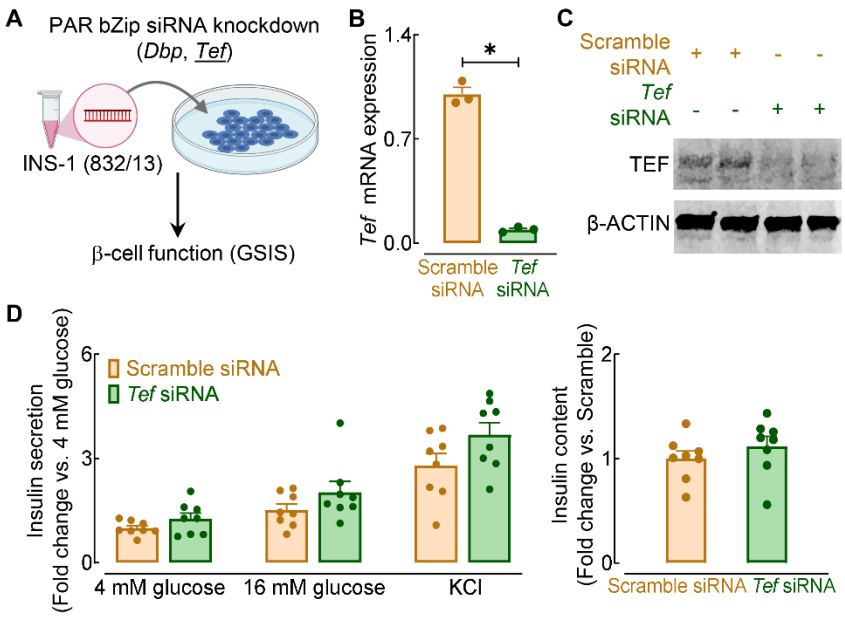

Fig. S9. siRNA knockdown of PAR bZip transcription factor Tef does not modulate glucose-stimulated insulin secretion or insulin content in β-cells. (A) Overview of study design. PAR bZip TFs (*Dbp* and *Tef*) were knocked down using siRNA in INS1(832/13) rat β-cells. *Tef* (highlighted) is profiled in the figure. **(B)** Quantitative PCR analysis of *Tef* mRNA expression in scramble siRNA and *Tef* siRNA treated β-cells. *p<.05 denotes statistical significance (unpaired, two-tailed Student's t-test; n=3 independent samples per group). **(C)** Representative western blot of TEF and β-actin expression in scramble siRNA (20nM scrambled siRNA) and *Tef* siRNA treated β-cells (n=2 independent experiments). **(D)** Glucose-stimulated insulin secretion (16mM glucose) and maximal insulin secretion (30mM KCl) of scramble siRNA and *Tef* siRNA treated cells normalized to basal insulin secretion at 4mM glucose (left). Total cell insulin content normalized to scramble siRNA control (right; p>.05, unpaired, two-tailed Student's t-test; n=8 independent samples per group). All values reported represent mean ± SEM.

Data S1. ARSER analysis of 525 transcripts rhythmic in CON and CD-tRF islets and arhythmic under CD.